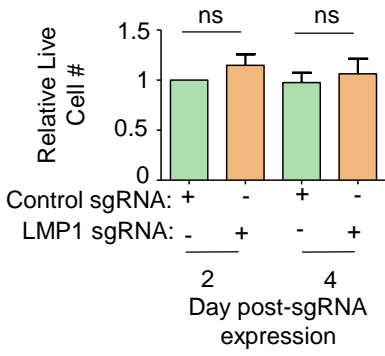
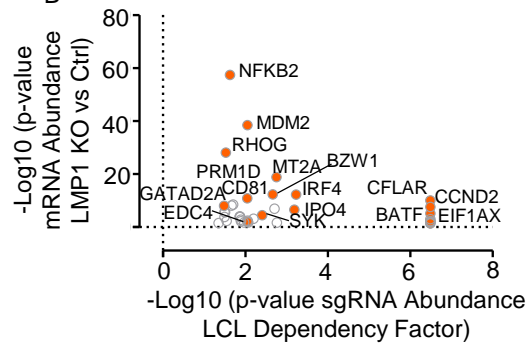


A



B



C

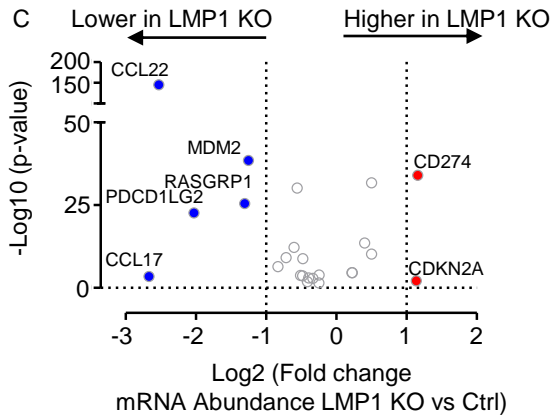


### Fig. S1. Characterization of LMP1 KO effects on GM12878 LCL target gene regulation.

(A) Relative mean + standard deviation (SD) live cell numbers from CellTitreGlo analysis of n=3 replicates of Cas9+ GM12878 LCLs, transduced with lentiviruses that expressed control or LMP1 sgRNAs and puromycin selected, for 2 versus 4 days.

(B) Scatter plot analysis cross-comparing the significance of changes in LCL dependency factor expression upon GM12878 LMP1 KO versus the CRISPR screen significance score for selection against sgRNAs in LCL vs Burkitt dependency factor analysis (25). Shown on the Y-axis are  $-\log_{10}$  transformed P-values from RNAseq analysis of GM12878 LCLs transduced with lentiviruses expressing LMP1 versus control sgRNA (as in **Fig. 1F**), versus  $-\log_{10}$  transformed P-values from CRISPR LCL vs Burkitt cell dependency factor analysis (25). Higher Y-axis scores indicate more significant differences in expression for the indicated genes in GM12878 with LMP1 vs control sgRNA. Higher X-axis scores indicate a stronger selection against sgRNA targeting the indicated genes in GM12878 LCLs versus P3HR1 Burkitt cells over 21 days of cell culture. Shown are genes with  $p < 0.05$  in both analyses.

(C) Volcano plot analysis visualizing KEGG Hodgkin lymphoma pathway gene  $-\log_{10}$  (P-value) on the y-axis versus  $\log_2$  transformed fold change in mRNA abundances on the x-axis of GM12878 genes in cells expressing LMP1 versus control sgRNA (as in **Fig. 1F**). P-value  $< 0.05$  and  $> 2$ -fold change mRNA abundance cutoffs were used.

A

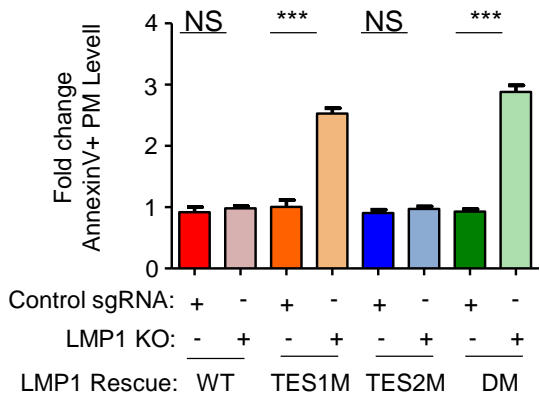


**Fig. S2. Loss of TES1 but not TES2 signaling triggers LCL apoptosis.**

Mean  $\pm$  SD of fold change plasma membrane Annexin V values from n=3 independent experiments, using GM12878 with the indicated control or LMP1 sgRNA and rescue cDNA expression. Values in GM12878 with control sgRNA and no LMP1 rescue cDNA were set to 1.

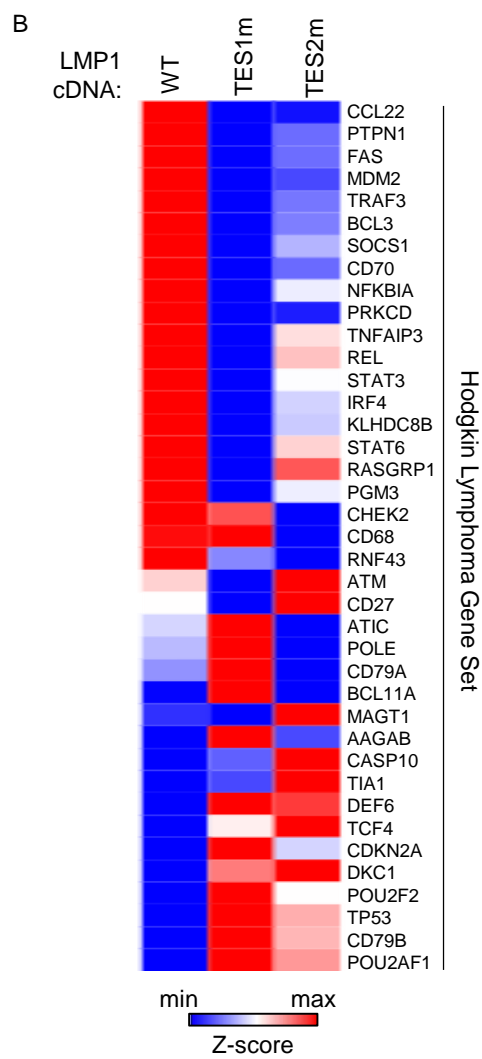
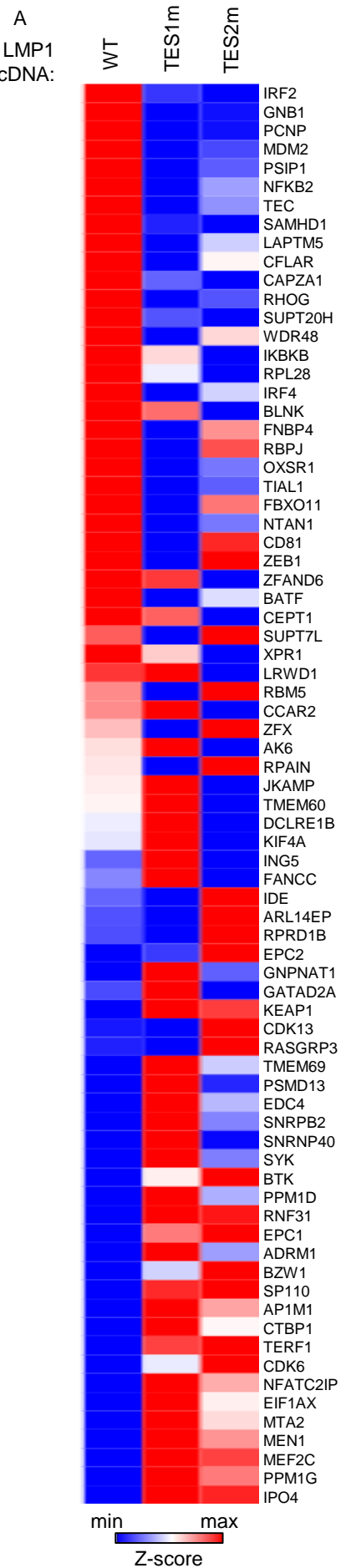


**Figure S3. Characterization of TES1 vs TES2 LCL dependency factor and Hodgkin lymphoma pathway targets.**

(A) Heatmap analysis of CRISPR defined LCL dependency factor gene relative row Z-scores from RNAseq of GM12878 expressing LMP1 sgRNA and the indicated rescue cDNA, as in **Fig. 3**. The Z-score scale is shown at bottom, where blue and red colors indicate lower versus higher relative expression, respectively. Two-way ANOVA P-value cutoff of  $<0.05$  and  $>2$ -fold gene expression cutoffs were used.

(B) Heatmap analysis of KEGG Hodgkin Lymphoma pathway gene relative row Z-scores from RNAseq of GM12878 expressing LMP1 sgRNA and the indicated rescue cDNA, as in **Fig. 3**. Two-way ANOVA P-value cutoff of  $<0.05$  and  $>2$ -fold gene expression cutoffs were used.

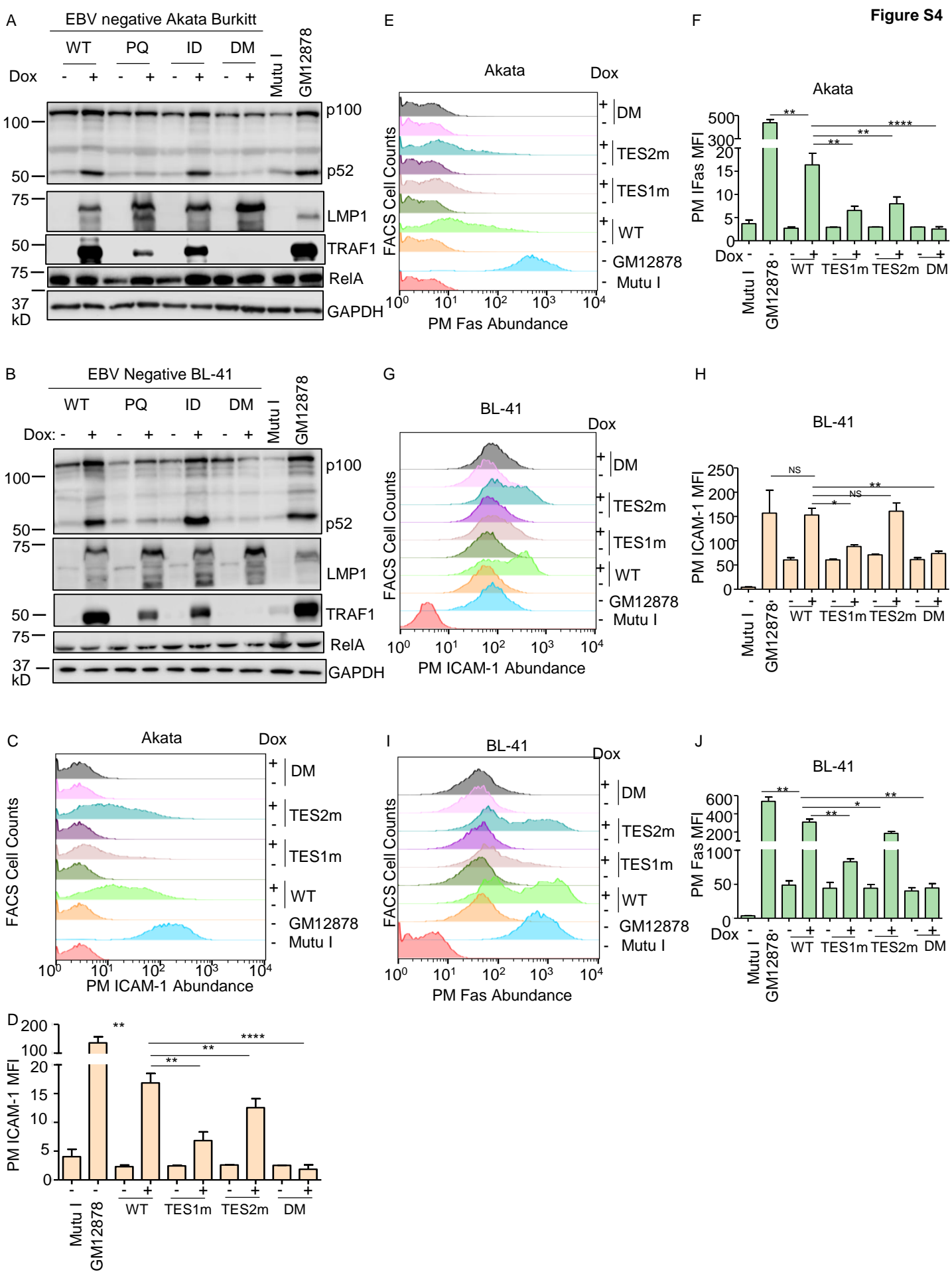


**Fig. S4. Validation of LMP1 WT, TES1m, TES2m and DM conditional expression system in EBV-negative Akata Burkitt B-cells.**

(A) Immunoblot analysis of WCL from Akata cells induced for LMP1 WT, TES1m, TES2m or DM expression by addition of 250 ng/ml doxycycline (Dox) for 24 hours, as indicated. For cross-comparison, WCL from equal numbers of Mutu I Burkitt lymphoma (latency I, lacks LMP1 expression) and GM12878 were also included at right. Blots are representative of n = 3 experiments.

(B) Immunoblot analysis of WCL from BL-41 cells induced for WT, TES1m, TES2m or DM LMP1 by addition of 250 ng/ml Dox for 24 hours, as indicated. For cross-comparison, WCL from equal numbers of Mutu I Burkitt and GM12878 were also included at right. Blots are representative of n = 3 experiments.

(C) FACS analysis of plasma membrane (PM) ICAM-1 abundance in Akata cells induced for LMP1 by 250 ng/ml Dox for 24 hours, as indicated. Y-axis are histogram cell counts, X-axis represents PM ICAM-1 abundance. For comparison, levels in GM12878 LCLs or latency I Mutu I Burkitt cells are shown.

(D) PM ICAM-1 Mean Fluorescence Intensity (MFI) + standard deviation (SD) from n=3 replicates in Akata cells with the indicated LMP1 expression, as in (C). p-values were determined by one-sided Fisher's exact test. \*\*p<0.001, \*\*\*p<0.0001.

(E) FACS analysis of PM Fas abundance in Akata cells induced for LMP1 by 250ng/ml of Dox for 24 hours as indicated. For comparison, GM12878 LCLs or latency I Mutu I Burkitt cells were also analyzed.

(F) PM Fas MFI + SD from n=3 replicates in Akata cells with the indicated LMP1 expression, as in (E). P-values were determined by one-sided Fisher's exact test. \*\*p<0.001, \*\*\*p<0.0001.

(G) FACS analysis of PM ICAM-1 in BL-41 cells induced for LMP1 expression by 250ng/ml Dox for 24 hours, as indicated. For comparison, GM12878 and Mutu I were also analyzed. p-values were determined by one-sided Fisher's exact test. \*\*p<0.001, \*\*\*p<0.0001.

(H) PM ICAM-1 MFI + SD from n=3 replicates in BL-41 cells with the indicated LMP1 expression, as in (G). P-values were determined by one-sided Fisher's exact test. \*\*p<0.001, \*\*\*p<0.0001.

(I) FACS analysis of PM Fas levels in BL-41 cells induced for LMP1 expression by 250 ng/ml dox for 24 hours, as indicated. GM12878 and Mutu I were analyzed for cross-comparison. p-values were determined by one-sided Fisher's exact test. \*\*p<0.001, \*\*\*p<0.0001.

(J) PM Fas MFI + SD from n=3 replicates of BL-41-LMP1 with the indicated LMP1 expression, as in (I). Mutu I and GM12878 were analyzed for comparison. p-values were determined by one-sided Fisher's exact test. \*\*p<0.001, \*\*\*p<0.0001.



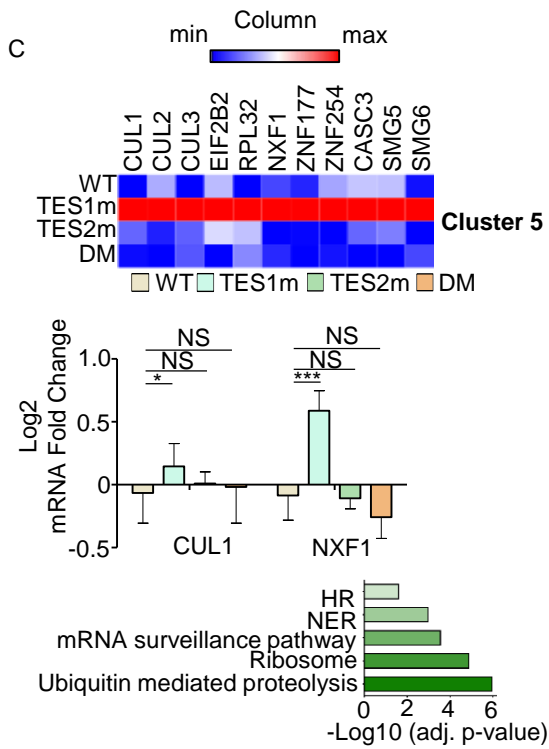
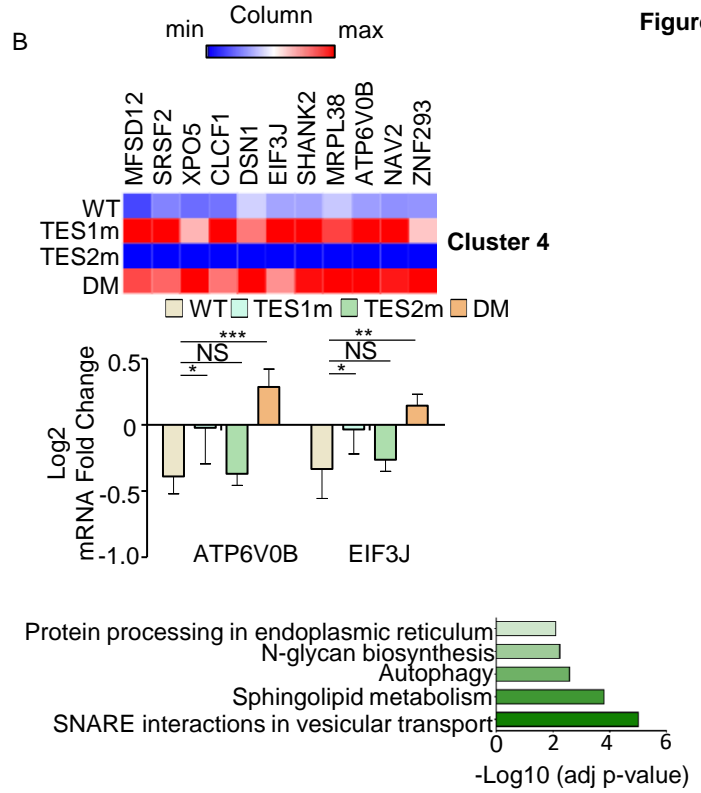
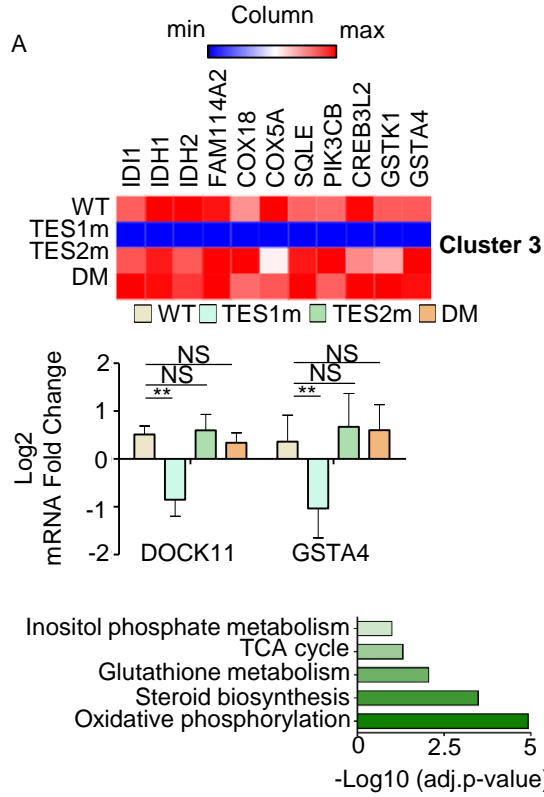


**Fig. S5. Characterization of host genome-wide Akata B-cell LMP1 target genes, related to Figure 4.**

(A) Heatmaps of representative **Figure 4** Cluster 3 differentially regulated genes (top), with column maximum colored red and minimum colored blue, as shown by the scalebar. Also shown are expression values of two representative Clusters 3 genes (lower left) and Enrichr analysis of KEGG pathways most significantly enriched Cluster 3 gene sets (lower right). p-values were determined by one-sided Fisher's exact test. \*\* $p < 0.01$ .

(B) Heatmaps of representative **Figure 4** Cluster 4 differentially regulated genes (top), with column maximum colored red and minimum colored blue, as shown by the scalebar. Also shown are expression values of two representative Clusters 4 genes (lower left) and Enrichr analysis of KEGG pathways most significantly enriched Cluster 4 gene sets (lower right). p-values were determined by one-sided Fisher's exact test. \* $p < 0.05$ , \*\* $p < 0.01$ , \*\*\* $p < 0.001$ .

(C) Heatmaps of representative **Figure 4** Cluster 5 differentially regulated genes (top), with column maximum colored red and minimum colored blue, as shown by the scalebar. Also shown are expression values of two representative Clusters 5 genes (lower left) and Enrichr analysis of KEGG pathways most significantly enriched Cluster 5 gene sets (lower right). p-values were determined by one-sided Fisher's exact test. \* $p < 0.05$ , \*\*\* $p < 0.001$ .

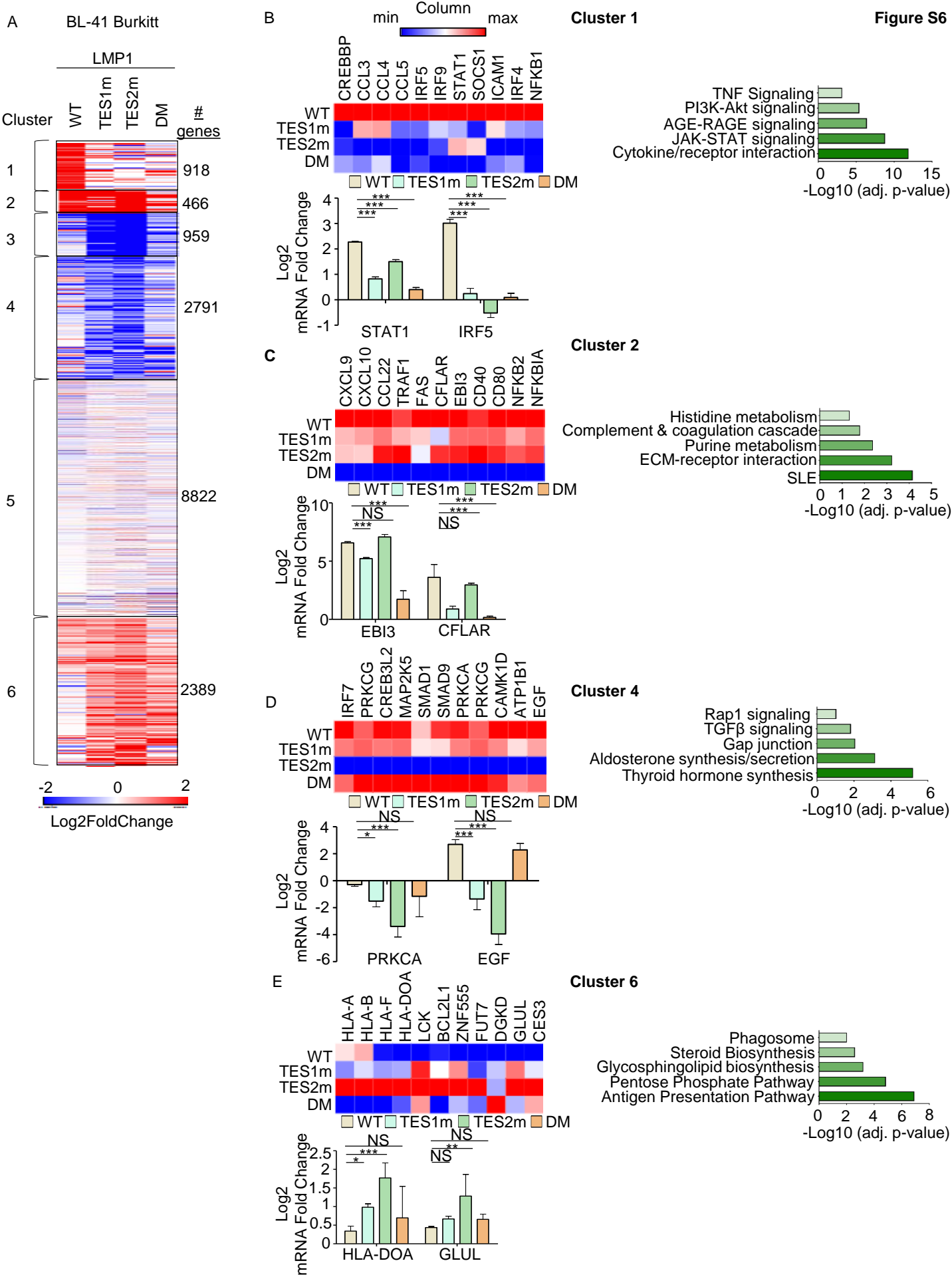


**Fig. S6. RNAseq analysis of BL-41 B-cell responses to WT, TES1, TES2 or DM LMP1.**

(A) K-means heatmap analysis of RNAseq datasets from n=3 replicates generated in EBV- BL-41 Burkitt cells with conditional LMP1 WT, TES1m, TES2m or DM expression induced by 250 ng/ml doxycycline for 24 hours. The heatmap visualizes host gene Log2 Fold change across the four conditions, divided into six clusters. A two-way ANOVA P value cutoff of <0.01 and >2-fold gene expression were used. # of genes in each cluster is indicated at right.

(B) Heatmaps of representative Cluster 1 differentially regulated genes (top), with column maximum (max) colored red and minimum (min) colored blue, as shown by the scalebar. Also shown are expression values of two representative Cluster 1 genes (lower left) and Enrichr analysis of KEGG pathways significantly enriched in Cluster 1 gene sets (lower right). p-values were determined by one-sided Fisher's exact test. \*\*\*p<0.001.

(C) Heatmaps of representative Cluster 2 differentially regulated genes (top). Also shown are expression values of two representative Cluster 2 genes (lower left) and Enrichr analysis of KEGG pathways significantly enriched in Cluster 2 gene sets (lower right). p-values were determined by one-sided Fisher's exact test. \*\*\*p<0.001.

(D) Heatmaps of representative Cluster 4 differentially regulated genes (top). Also shown are expression values of two representative Cluster 4 genes (lower left) and Enrichr analysis of KEGG pathways significantly enriched in Cluster 4 gene sets (lower right). p-values were determined by one-sided Fisher's exact test. \*p<0.05, \*\*\*p<0.001.

(E) Heatmaps of representative Cluster 6 differentially regulated genes (top). Also shown are expression values of two representative Cluster 6 genes (lower left) and Enrichr analysis of KEGG pathways significantly enriched in Cluster 6 gene sets (lower right). p-values were determined by one-sided Fisher's exact test. \*p<0.05, \*\*p<0.01, \*\*\*p<0.001.

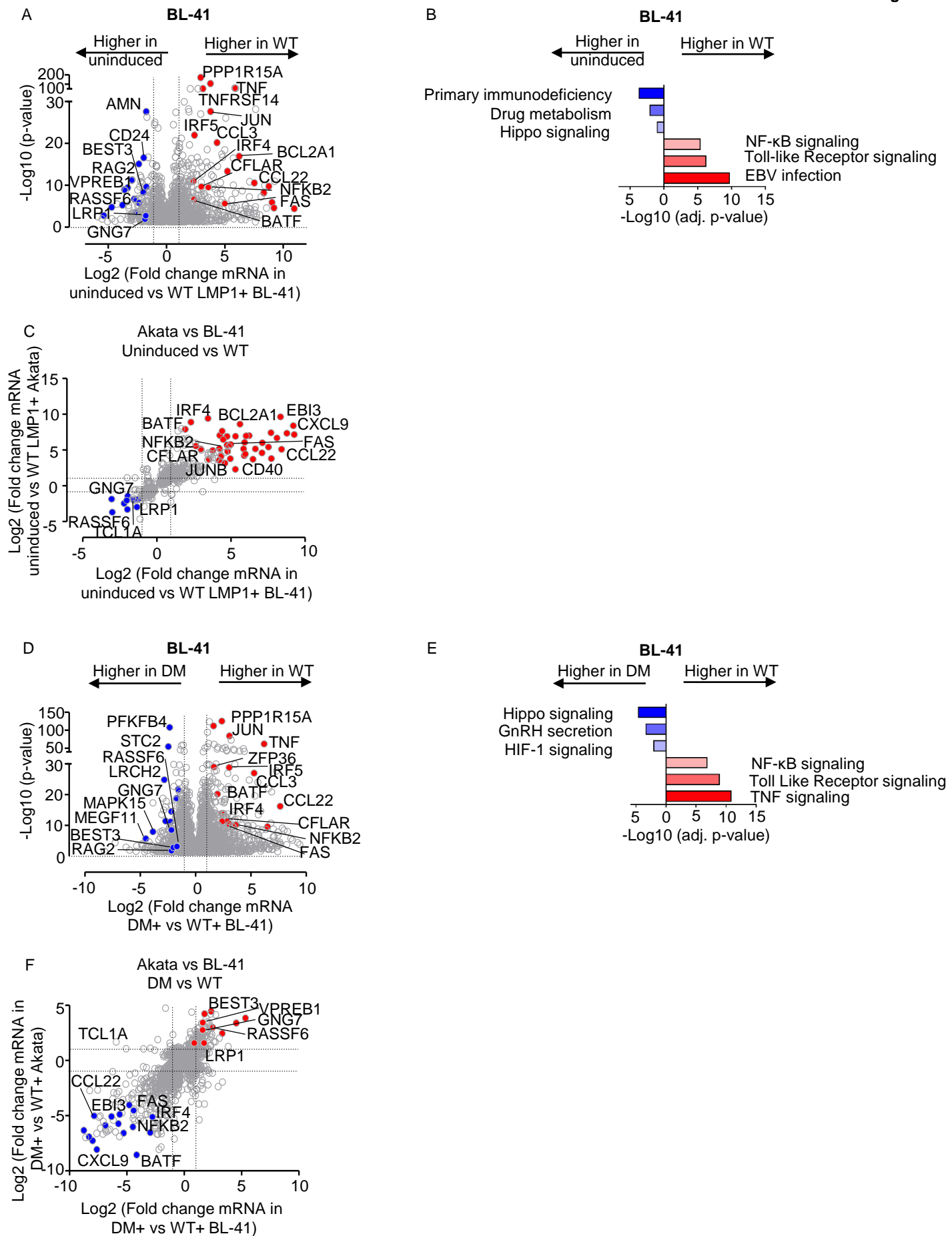


**Fig. S7. Cross-comparison of WT and DM LMP1 effects on Akata vs BL-41 transcriptomes.**

(A) Volcano plot analysis of host transcriptome-wide genes differentially expressed in BL-41 cells conditionally induced for WT LMP1 expression for 24h by 250 ng/ml Dox versus in mock induced cells. Higher X-axis fold changes indicate genes more highly expressed in cells with WT LMP1 expression, whereas lower X-axis fold changes indicate higher expression in cells mock induced for LMP1. Data are from n=3 RNAseq datasets.

(B) Enrichr analysis of KEGG pathways most highly enriched in RNAseq data as in (A) amongst genes more highly expressed in BL-41 with WT LMP1 (red) vs amongst genes more highly expressed with mock LMP1 induction (blue).

(C) Volcano plot cross-comparison of Log<sub>2</sub> transformed fold change of host mRNA levels in BL-41 cells (X-axis) versus Akata cells (Y-axis) uninduced versus induced for WT LMP1 by 250 ng/ml Dox for 24 hours. Selected genes highly WT LMP1 induced in both Burkitt contexts are highlighted in red, whereas selected genes suppressed by LMP1 in both Burkitt contexts are highlighted in blue.

(D) Volcano plot analysis of host transcriptome-wide genes differentially expressed in BL-41 cells conditionally induced for DM versus WT LMP1 expression for 24h by 250 ng/ml Dox. Higher X-axis fold changes indicate genes more highly expressed in cells with WT LMP1 expression, whereas lower X-axis fold changes indicate higher expression in cells induced for DM LMP1. Data are from n=3 RNAseq datasets.

(E) Enrichr analysis of KEGG pathways most highly enriched in RNAseq data as in (D) amongst genes more highly expressed in BL-41 with WT LMP1 (red) vs amongst genes more highly expressed with DM LMP1 induction (blue).

(F) Volcano plot cross-comparison of Log<sub>2</sub> transformed fold change of host mRNA levels in BL-41 cells (X-axis) versus Akata cells (Y-axis) induced for DM versus WT LMP1 by 250 ng/ml Dox for 24 hours. Selected genes highly WT LMP1 induced in both Burkitt contexts relative to levels in cells with DM LMP1 expression are highlighted in red, whereas selected genes suppressed by WT LMP1 in both Burkitt contexts are highlighted in blue.

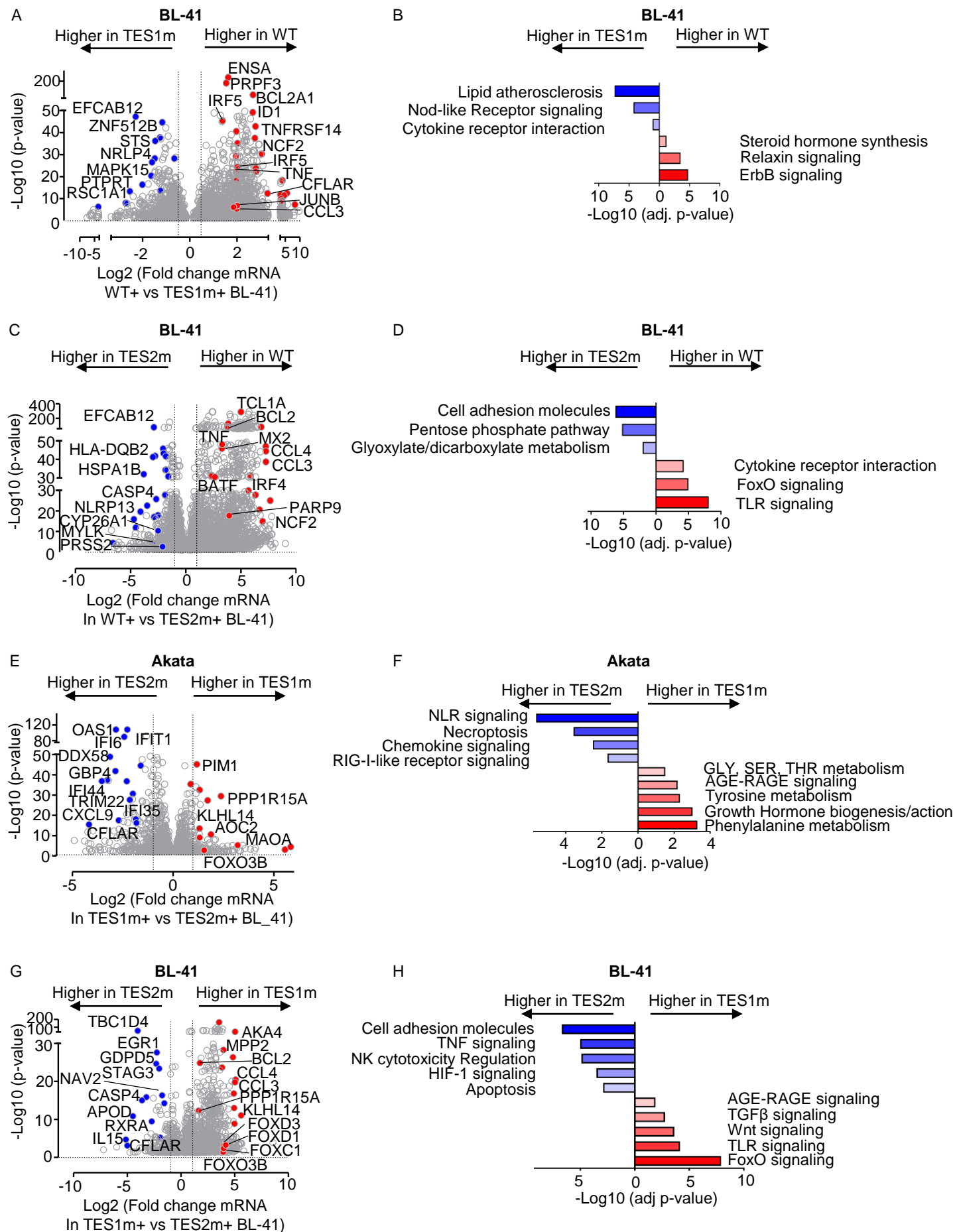


**Fig. S8. Cross-comparison of TES1 and TES2 LMP1 effects on Akata vs BL-41 transcriptomes.**

A) Volcano plot analysis of host transcriptome-wide genes differentially expressed in BL-41 cells conditionally induced for TES1m vs WT LMP1 expression for 24h by 250 ng/ml Dox. Higher X-axis fold changes indicate genes more highly expressed in cells with WT LMP1 expression, whereas lower X-axis fold changes indicate higher expression induced for TES1m LMP1. Data are from n=3 RNAseq datasets.

(B) Enrichr analysis of KEGG pathways most highly enriched in RNAseq data as in (A) amongst genes more highly expressed in BL-41 with WT LMP1 (red) vs amongst genes more highly expressed with TES1m LMP1 induction (blue).

(C) Volcano plot analysis of host transcriptome-wide genes differentially expressed in BL-41 cells conditionally induced for TES2m vs WT LMP1 expression for 24h by 250 ng/ml Dox. Higher X-axis fold changes indicate genes more highly expressed in cells with WT LMP1 expression, whereas lower X-axis fold changes indicate higher expression induced for TES2m LMP1. Data are from n=3 RNAseq datasets.

(D) Enrichr analysis of KEGG pathways most highly enriched in RNAseq data as in (A) amongst genes more highly expressed in BL-41 with WT LMP1 (red) vs amongst genes more highly expressed with TES2m LMP1 induction (blue).

(E) Volcano plot analysis of host transcriptome-wide genes differentially expressed in Akata cells conditionally induced for TES1m vs TES2m LMP1 expression for 24h by 250 ng/ml Dox. Higher X-axis fold changes indicate genes more highly expressed in cells with TES1m LMP1 expression, whereas lower X-axis fold changes indicate higher expression induced for TES2m LMP1. Data are from n=3 RNAseq datasets.

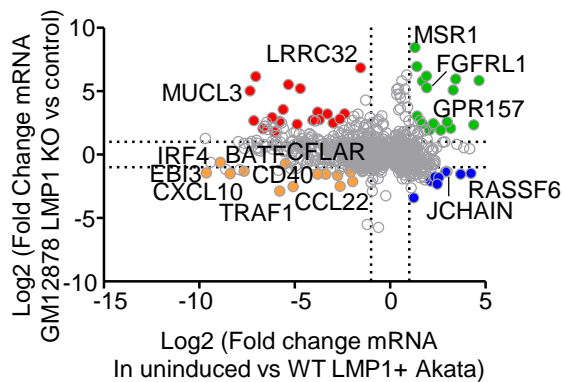
(F) Enrichr analysis of KEGG pathways most highly enriched in RNAseq data as in (E) amongst genes more highly expressed in Akata with TES1m LMP1 (red) vs amongst genes more highly expressed with TES2m LMP1 induction (blue).

(G) Volcano plot analysis of host transcriptome-wide genes differentially expressed in BL-41 cells conditionally induced for TES1m vs TES2m LMP1 expression for 24h by 250 ng/ml Dox. Higher X-axis fold changes indicate genes more highly expressed in cells with TES1m LMP1 expression, whereas lower X-axis fold changes indicate higher expression induced for TES2m LMP1. Data are from n=3 RNAseq datasets.

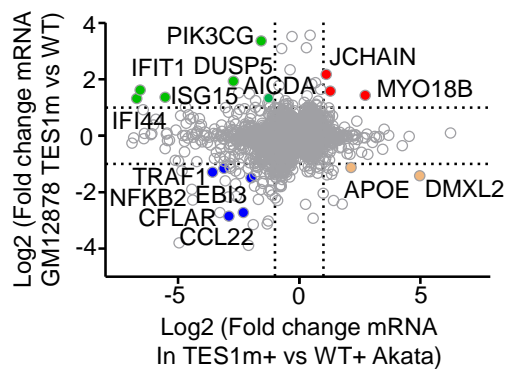
(H) Enrichr analysis of KEGG pathways most highly enriched in RNAseq data as in (G) amongst genes more highly expressed in BL-41 with TES1m LMP1 (red) vs amongst genes more highly expressed with TES2m LMP1 induction (blue).



A



B



C

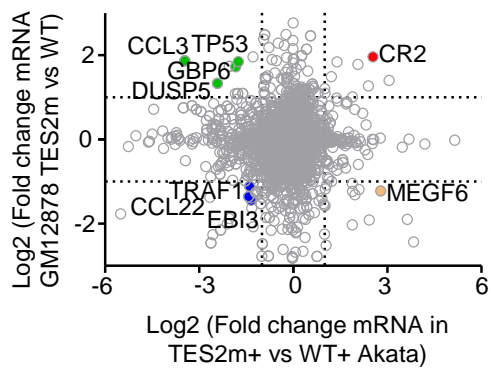


**Figure S9. Cross-comparison of host genes differentially expressed upon perturbation of LCL LMP1 versus upon LMP1 induction in Akata cells.**

(A) Volcano plot analysis of host genes differentially expressed upon WT LMP1 induction in Akata (X-axis) versus upon LMP1 KO in GM12878 (Y-axis). Shown are Log<sub>2</sub> transformed mRNA fold change values for Akata cells mock induced versus induced for LMP1 WT expression for 24 hours (X-axis) versus upon expression of LMP1 vs control sgRNA in GM12878 for 48 hours. Genes more highly expressed in mock-induced Akata have higher x-axis values, whereas genes more highly expressed in Akata induced for WT LMP1 have lower x-axis values. Likewise, genes with higher expression with control sgRNA expression have higher y-axis values, whereas genes with lower expression in GM12878 with LMP1 KO have lower Y-axis values. P value <0.05 and >2-fold gene expression cutoffs were used.

(B) Volcano plot analysis of host genes differentially expressed upon TES1m vs WT LMP1 induction in Akata (X-axis) versus upon rescue of LMP1 KO GM12878 with TES1m versus WT LMP1 (Y-axis). Shown are Log<sub>2</sub> transformed mRNA fold change values for Akata cells induced for TES1m versus WT LMP1 expression for 24 hours (X-axis) versus upon rescue of GM12878 LMP1 KO with TES1m vs WT LMP1 cDNA, as in **Fig 3**. Genes more highly expressed in Akata with TES1m than WT LMP1 expression have higher x-axis values, whereas genes more highly expressed in Akata induced for WT LMP1 than TES1m have lower x-axis values. Likewise, GM12878 genes with higher expression with TES1m rescue have higher y-axis values, whereas genes with lower expression in GM12878 with TES1m than WT rescue have lower Y-axis values. P value <0.05 and >2-fold gene expression cutoffs were used.

(C) Volcano plot analysis of host genes differentially expressed upon TES2m vs WT LMP1 induction in Akata (X-axis) versus upon rescue of LMP1 KO GM12878 with TES2m versus WT LMP1 (Y-axis). Shown are Log<sub>2</sub> transformed mRNA fold change values for Akata cells induced for TES2m versus WT LMP1 expression for 24 hours (X-axis) versus upon rescue of GM12878 LMP1 KO with TES2m vs WT LMP1 cDNA, as in **Fig 3**. Genes more highly expressed in Akata with TES2m than WT LMP1 expression have higher x-axis values, whereas genes more highly expressed in Akata induced for WT LMP1 than TES2m have lower x-axis values. Likewise, GM12878 genes with higher expression with TES2m rescue have higher y-axis values, whereas genes with lower expression in GM12878 with TES2m than WT rescue have lower Y-axis values. P value <0.05 and >2-fold gene expression cutoffs were used.

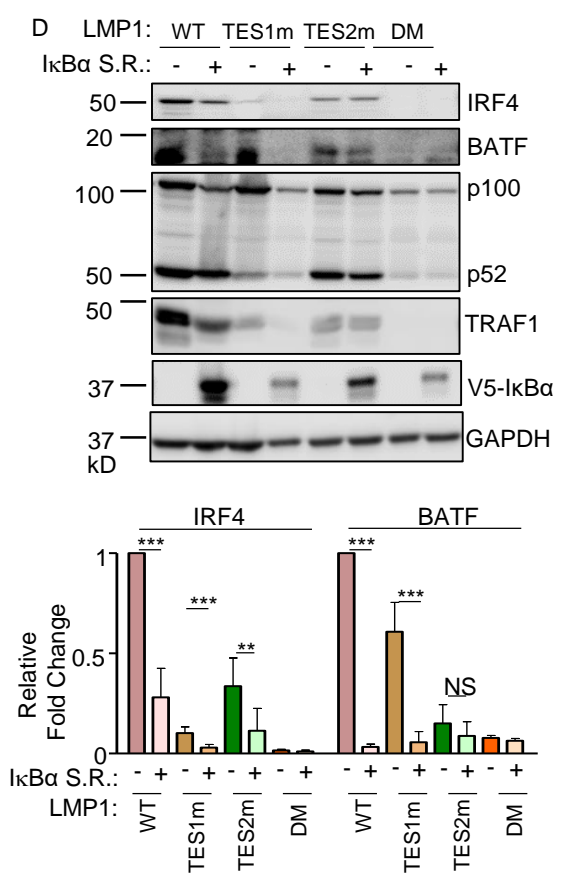
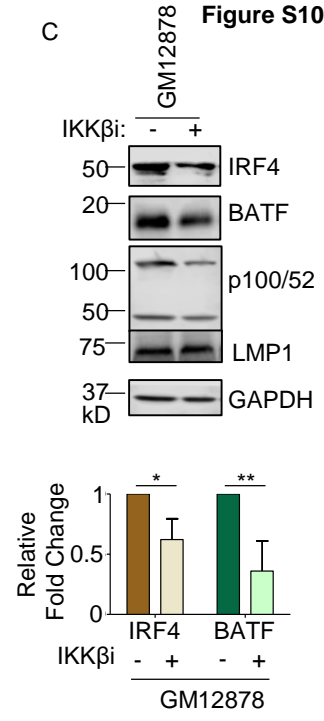
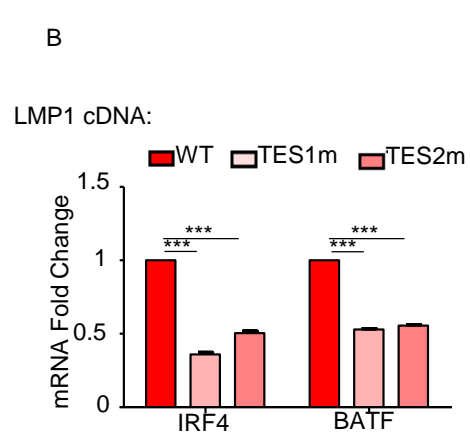
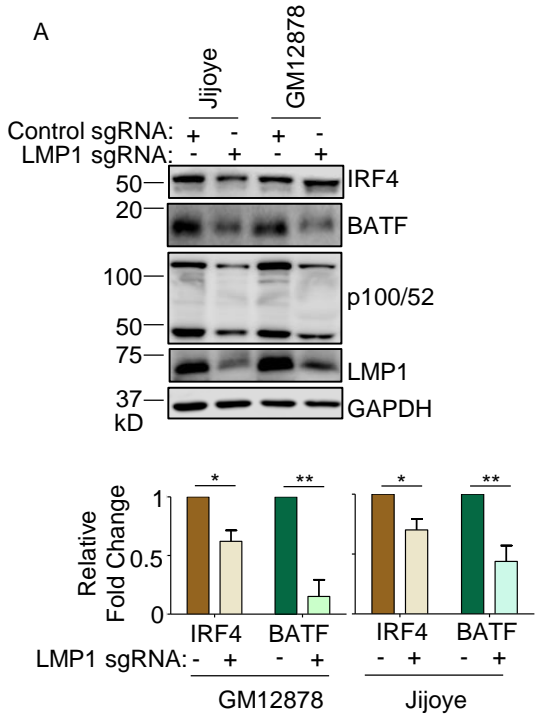


**Fig. S10. Roles of TES1 and TES2 canonical NF- $\kappa$ B pathways in BATF and IRF4 induction.**

(A) Immunoblot analysis of WCL from latency III Jijoye Burkitt cells or GM12878 LCL expressing LMP1 targeting sgRNA, as indicated. Shown below are relative fold changes + SD from n=3 replicates of IRF4 or BATF vs GAPDH load control densitometry values, with values in sgRNA control expressing cells set to 1. P-values were determined by one-sided Fisher's exact test. \*\*p<0.001, \*\*\*p<0.0001.

(B) Relative +SD BATF and IRF4 mRNA levels from n=3 RNAseq replicates from LMP1 KO GM12878 with TES1m, TES2m or WT LMP1 rescue cDNA expression, as in Fig 3-4. BATF or IRF4 levels in cells with WT LMP1 rescue were defined as 1. \*\*\*p<0.0001.

(C) Immunoblot analysis of WCL from GM12878 LCLs treated with vehicle control or 1  $\mu$ M IKK $\beta$  inhibitor VIII for 24 hours. Shown below are relative foldchanges + SD from n=3 replicates of IRF4 or BATF vs GAPDH load control densitometry values. Levels in vehicle control treated WT LMP1 expressing cells were set to 1. P-values were determined by one-sided Fisher's exact test. \*\*p<0.001, \*\*\*p<0.0001.

(D) Immunoblot analysis of WCL from Akata cells induced for the indicated LMP1 construct expression, either without or together with an I $\kappa$ B $\alpha$  super-repressor (I $\kappa$ B $\alpha$ -S.R.) that blocks canonical NF- $\kappa$ B signaling. Shown below are relative foldchanges + SD of IRF4 or BATF vs GAPDH load control densitometry values from n=3 replicates, with values in cells expressing WT LMP1 but not I $\kappa$ B $\alpha$ - set to 1. P-values were determined by one-sided Fisher's exact test. \*\*p<0.001, \*\*\*p<0.0001.

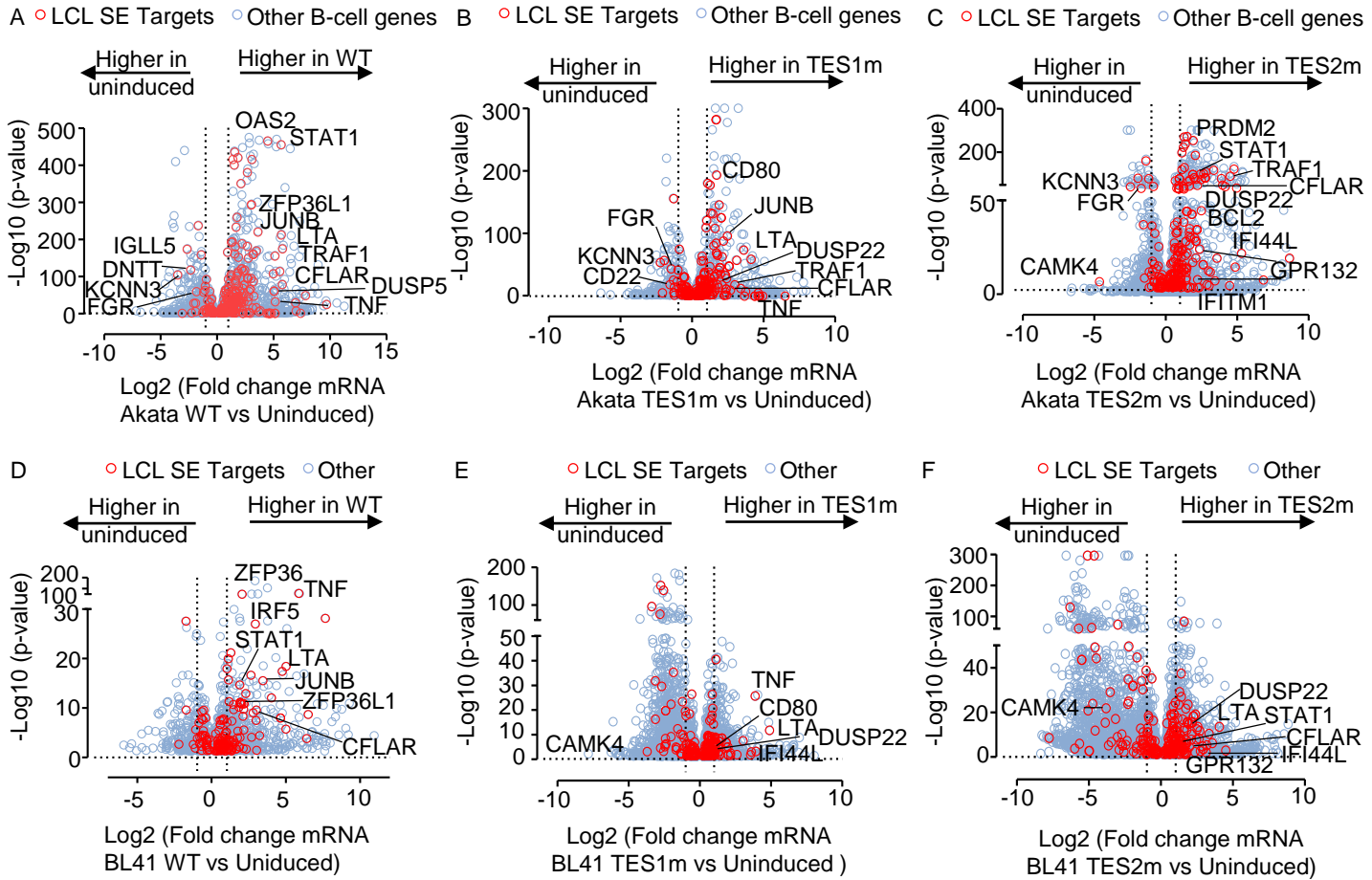


**Figure S11. LMP1 TES1 and TES2 roles in EBV super-enhancer target gene regulation in Akata and BL-41 Burkitt B-cells.**

- (A) Volcano plot analysis of Akata RNA-seq, comparing mRNA values in cells induced for LMP1 WT vs. mock-induced for 24 hours. SE targeted genes highlighted by red circles and other B-cell genes indicated by blue circles. P value  $<0.05$  and  $>2$ -fold gene expression cutoffs were used.
- (B) Volcano plot analysis of Akata RNA-seq, comparing mRNA values in cells induced for LMP1 TES1m vs. mock-induced for 24 hours. SE targeted genes highlighted by red circles and other B-cell genes indicated by blue circles. P value  $<0.05$  and  $>2$ -fold gene expression cutoffs were used.
- (C) Volcano plot analysis of Akata RNA-seq, comparing mRNA values in cells induced for LMP1 TES2m vs. mock-induced for 24 hours. SE targeted genes highlighted by red circles and other B-cell genes indicated by blue circles. P value  $<0.05$  and  $>2$ -fold gene expression cutoffs were used.
- (D) Volcano plot analysis of BL-41 RNA-seq, comparing mRNA values in cells induced for LMP1 WT vs. mock-induced for 24 hours. SE targeted genes highlighted by red circles and other B-cell genes indicated by blue circles. P value  $<0.05$  and  $>2$ -fold gene expression cutoffs were used.
- (E) Volcano plot analysis of BL-41 RNA-seq, comparing mRNA values in cells induced for LMP1 TES1m vs. mock-induced for 24 hours. SE targeted genes highlighted by red circles and other B-cell genes indicated by blue circles. P value  $<0.05$  and  $>2$ -fold gene expression cutoffs were used.
- (F) Volcano plot analysis of BL-41 RNA-seq, comparing mRNA values in cells induced for LMP1 TES2m vs. mock-induced for 24 hours. SE targeted genes highlighted by red circles and other B-cell genes indicated by blue circles. P value  $<0.05$  and  $>2$ -fold gene expression cutoffs were used.